Exp.-Nr.: A1/2–99
Eingang:
an PAC:

Mainz Microtron MAMI

Collaboration A1: "Virtual Photons"

Spokesperson: R. Neuhausen

Proposal for an Experiment

Measurement of the neutron electric form factor in $\mathrm{D}(\vec{\mathrm{e}}, \mathrm{e}'\vec{\mathrm{n}})\mathrm{p}$ at $Q^2 = 0.6$ and 0.8 $(\mathrm{GeV}/c)^2$

Collaborators:

P. Bartsch, D. Baumann, R. Böhm, S. Derber, M. Ding, M. O. Distler, I. Ewald, J. Friedrich, J. M. Friedrich, S. Grözinger, P. Jennewein, K. W. Krygier, H. Merkel, K. Merle, P. Merle, U. Müller*, R. Neuhausen, Th. Pospischil, A. Radoselovics, J. Sanner, H. Schmieden*, M. Seimetz, O. Strähle, A. Süle, Th. Walcher, M. Weis
(Institut für Kernphysik, Univ. Mainz, 55099 Mainz, Germany)

J. R. M. Annand, D. G. Ireland, R. O. Owens, G. Rosner
(Dept. of Physics and Astron., Univ. of Glasgow, Glasgow G12 8QQ, Scotland, UK)

*Contact Persons

Abstract:

We propose to measure the neutron electric form factor, $G_{E,n}$, in the $\mathrm{D}(\vec{\mathrm{e}}, \mathrm{e}'\vec{\mathrm{n}})\mathrm{p}$ reaction at $Q^2 = 0.6$ and 0.8 $(\mathrm{GeV}/c)^2$. This will be the first model-independent measurement of $G_{E,n}$ by doubly polarized quasi-free scattering off deuterium in this range of Q^2. It will thus supplement the previous MAMI results.

1 Introduction

During the last two years, a model independent measurement of the neutron electric form factor, $G_{E,n}$, became possible through double polarization experiments of the type $^3\vec{\mathrm{He}}(\vec{\mathrm{e}},\mathrm{e}'\mathrm{n})\mathrm{pp}$ and $\mathrm{D}(\vec{\mathrm{e}},\mathrm{e}'\vec{\mathrm{n}})\mathrm{p}$. The results are summarized in Figure 1.

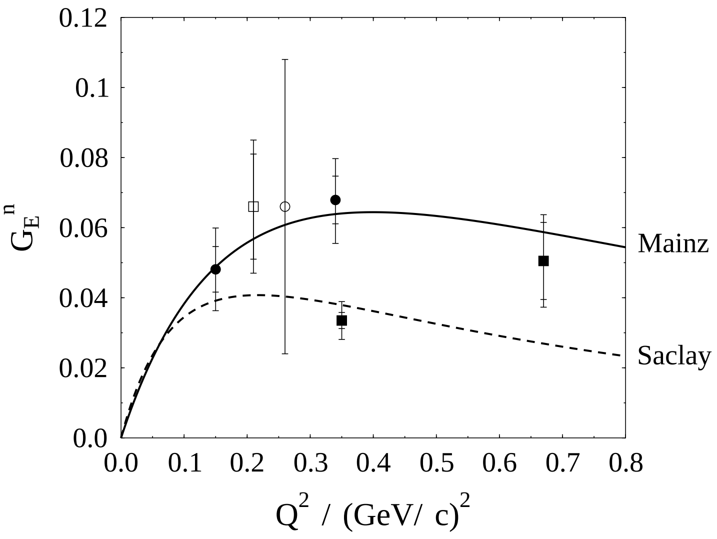

Figure 1: Results for G_E^n from double polarization experiments with Deuteron targets at MAMI (full circles) [1, 2], NIKHEF (open square) [3] and MIT/Bates (open circle) [4], and from experiments with polarized ^{3}He target at MAMI (full squares) [5, 6]. The full curve represents the new Mainz parametrization for G_E^n. For comparison the preferred parametrization from the unpolarized, elastic Saclay measurement [7] is displayed as broken line.

While the $^3\vec{\mathrm{He}}$ measurements cover the range of 4-momentum transfer $Q^2 = 0.31 - 0.67$ (GeV/c)^2 [5, 6], the D-experiments with recoil or target polarization are yet restricted to the range of $Q^2 = 0.15 - 0.34$ (GeV/c)^2 [1, 2, 3, 4]. The MAMI results yielded a new parametrization for $G_{E,n}$ [1]. It lies almost a factor of two above the so far favoured Saclay result, where the Paris potential was used for the extraction of $G_{E,n}$ from elastic e-D scattering [7]. The significant influence on the corresponding neutron charge distribution is illustrated in Figure 2.

Even in quasi-free electron scattering off the D, the final state interaction of the outgoing neutron is not negligible, in particular in the case of small Q^2, i.e. small relative kinetic energies between n and p in the final state. Based on calculations

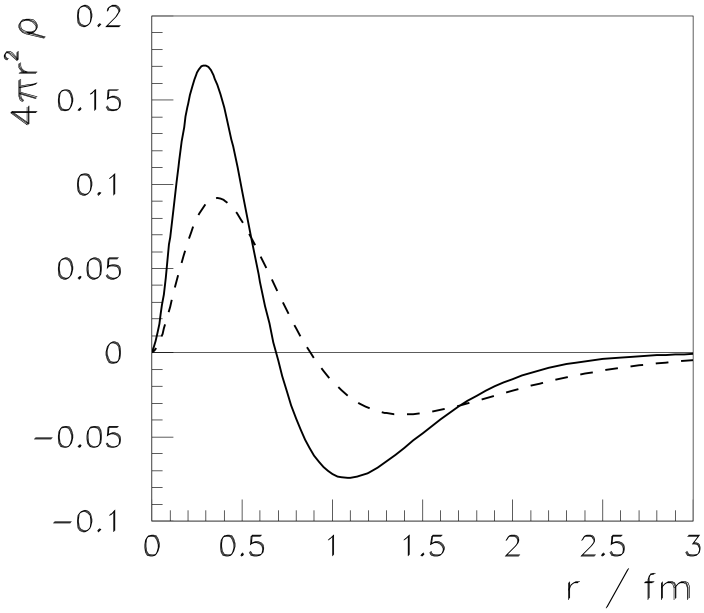

Figure 2: Neutron charge distribution from the Mainz (full) and the preferred Saclay (broken) G_E^n parametrization.

of H. Arenhövel [8], the FSI has been studied for the phase space acceptance of the MAMI experiments [1]. At $Q^2 = 0.15$ (GeV/c)^2, a 100% correction of the extracted $G_{E,n}$ is necessary, which drops to only 8% at $Q^2 = 0.34$ (GeV/c)^2.

First 3-body calculations for the $^3\vec{\mathrm{He}}(\vec{\mathrm{e}},\mathrm{e}'\mathrm{n})\mathrm{pp}$ reaction indicate, even at $Q^2 = 0.31$ (GeV/c)^2, a substantial FSI effect. It can explain most of the discrepancy between $G_{E,n}$ extracted from $^3\vec{\mathrm{He}}$ and D experiments. Final calculations are, however, not yet available. Therefore the $^3\vec{\mathrm{He}}$ results in Figure 1 are, in contrast to the D-results (except [4]), not FSI corrected.

A final confirmation of the Mainz parametrization which is independent of ambiguities in the FSI of the $^3\vec{\mathrm{He}}(\vec{\mathrm{e}},\mathrm{e}'\mathrm{n})\mathrm{pp}$ reaction requires a quasifree double polarization measurement with deuteron target in the range $Q^2 = 0.6 - 0.8$ (GeV/c)^2. These kinematics are still accessible at MAMI B.

2 Method

In order to measure the neutron electric form factor, $G_{E,n}$, in a model-independent way at the high Q^2, the same method that previously has been established at MAMI [2] will be used. A beam of polarized electrons hits an unpolarized, liquid deuterium target. In the quasielastic reaction $\mathrm{D}(\vec{\mathrm{e}},\mathrm{e}'\vec{\mathrm{n}})\mathrm{p}$ polarized neutrons are produced. The components of the outgoing neutron polarization carry the information on its electric and magnetic form factors. For free (e,n) scattering Arnold, Carlson and Gross obtained [9]:

$$\begin{aligned}
\mathcal{P}_x &= -hP_e \frac{2\sqrt{\tau(1+\tau)}\tan\frac{\vartheta_e}{2} G_E G_M}{G_E^2 + \tau G_M^2(1+2(1+\tau)\tan^2\frac{\vartheta_e}{2})} \\
\mathcal{P}_y &= 0 \\
\mathcal{P}_z &= hP_e \frac{2\tau\sqrt{1+\tau+(1+\tau)^2\tan^2\frac{\vartheta_e}{2}}\tan\frac{\vartheta_e}{2} G_M^2}{G_E^2 + \tau G_M^2(1+2(1+\tau)\tan^2\frac{\vartheta_e}{2})}
\end{aligned} \tag{1}$$

The coordinate frame (x, y, z) is defined relative to the electron scattering plane and the direction of the momentum transfer: $\hat{z} = \vec{q}/|\vec{q}|$, $\hat{y} = \vec{P}_{e_i} \times \vec{P}_{e_f}/|\vec{P}_{e_i} \times \vec{P}_{e_f}|$, $\hat{x} = \hat{y} \times \hat{z}$. The variable $\tau = Q^2/4M_n^2$ measures the negative squared 4-momentum transfer, Q^2, in units of the neutron mass, M_n. P_e denotes the degree of longitudinal electron beam polarization, and $h = \pm 1$ the electron helicity. For quasielastic scattering off a neutron bound in deuterium, Eqs. 1 are basically maintained [8] in the case of parallel kinematics, where the neutron is detected along the direction of the momentum transfer, $\vec{q}$. The ratio

$$\frac{\mathcal{P}_x}{\mathcal{P}_z} = -\frac{1}{\sqrt{\tau + \tau(1+\tau)\tan^2\frac{\vartheta_e}{2}}} \cdot \frac{G_{E,n}}{G_{M,n}} \tag{2}$$

is linear in $G_{E,n}$, and independent of the absolute value of P_e. The aim of the proposed experiment is to measure this ratio.

The overall setup of the proposed experiment is sketched in Figure 3. In order to tag the exclusive $(\vec{\mathrm{e}}, \mathrm{e}'\vec{\mathrm{n}})$ reaction, the scattered electrons and neutrons are detected in coincidence. Energy and angles of the scattered electrons are measured with high resolution in spectrometer A. This guarantees clean separation of π production events. An overdetermined reconstruction of the $\mathrm{D}(\vec{\mathrm{e}}, \mathrm{e}'\vec{\mathrm{n}})\mathrm{p}$ kinematics is achieved through the additional measurement of the time-of-flight of the neutrons and their hit position in a segmented scintillator 6 m away from the target. The neutron polarization can be analysed in the detector itself [10]. This requires to detect the neutrons a second time in a split wall, the two parts of which are positioned above and below the target (electron scattering plane). The polarimeter is described in more detail in section 3.

The angular distribution of the scattered neutrons follows

$$N^h(\Theta_n', \Phi_n') = \mathcal{L}^h \varepsilon(\Theta_n', \Phi_n')\sigma_0[1 + hP_e\mathcal{A}_{\text{eff}}(\Theta_n')(P_x \sin\Phi_n' + P_y\cos\Phi_n')], \tag{3}$$

where, $\varepsilon(\Theta_n', \Phi_n')$ is the detection efficiency of the second wall scintillators, as a function of the polar and azimuthal angles of the first wall scattering. $\mathcal{L}^h$ denotes the helicity specific luminosity and σ_0 the polarization-independent scattering cross-section. The effective analysing power, $\mathcal{A}_{\text{eff}}$, is a priori unknown because different reaction channels contribute in the scintillator material.

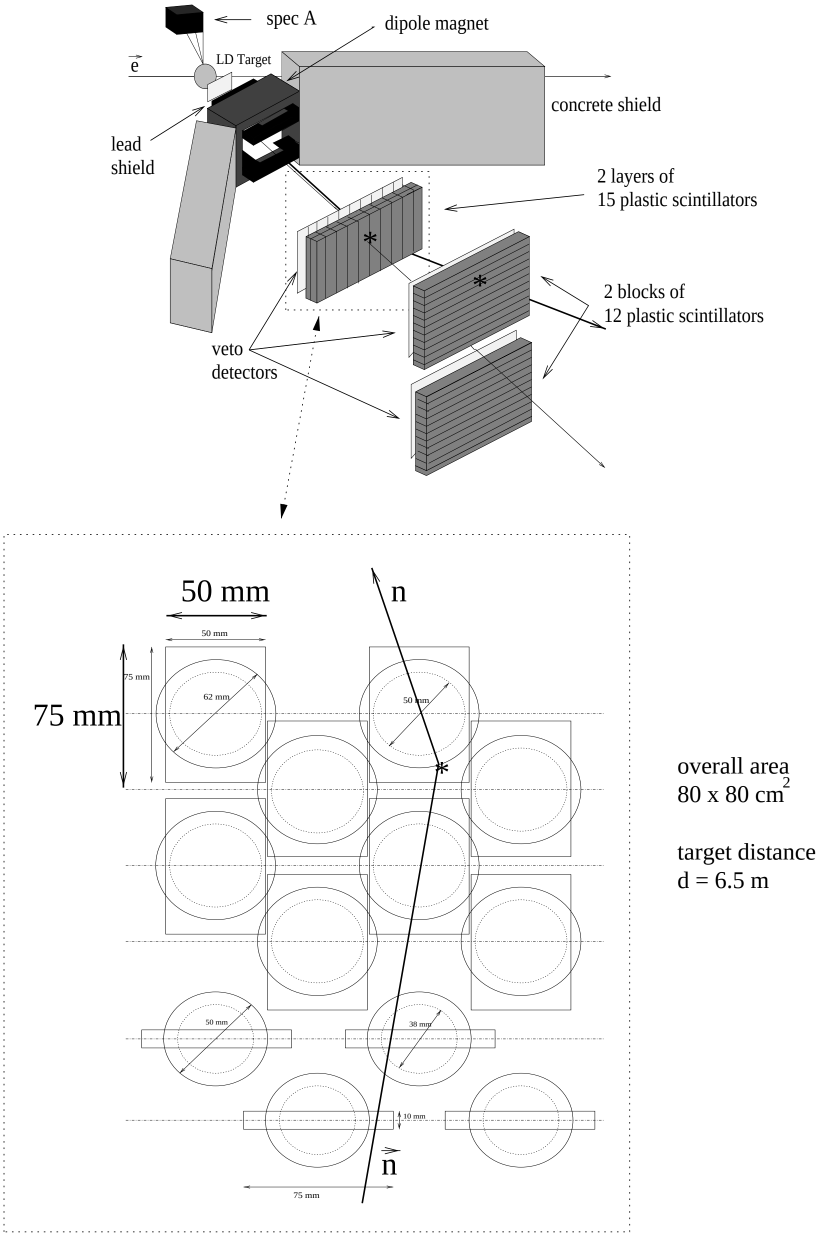

Figure 3: Detector setup and first wall of scintillators

Taking advantage of the fact that a reversal of the beam helicity h is equivalent to a shift of the azimuthal angle by 180°, the asymmetry

$$\begin{aligned} A &= \frac{\sqrt{N^+(\Phi'_n)N^-(\Phi'_n+180^\circ)}-\sqrt{N^+(\Phi'_n+180^\circ)N^-(\Phi'_n)}}{\sqrt{N^+(\Phi'_n)N^-(\Phi'_n+180^\circ)}+\sqrt{N^+(\Phi'_n+180^\circ)N^-(\Phi'_n)}} \\ &= P_e(\mathcal{A}^t_{\rm eff}P_x\sin\Phi'_n+\mathcal{A}^n_{\rm eff}P_y\cos\Phi'_n) \end{aligned} \tag{4}$$

can be constructed in a way independent of $\mathcal{L}^h, \varepsilon$, and σ_0. Here $N^\pm(\Phi'_n)$ is the count rate on the second wall of scintillators.

It has been demonstrated that the remaining problem of analysing power calibration of the polarimeter can be avoided by rotating the direction of the neutron spin in an external magnetic field [2]. In case of a field perpendicular to the neutron trajectory, the precession angle is proportional to the integrated field strength,

$$\chi = \frac{2\mu_n}{\hbar c}\cdot\beta_n^{-1}\int B\,dl = \frac{-35.02^\circ}{\rm Tm}\cdot\beta_n^{-1}\int B\,dl \quad . \tag{5}$$

In the proposed experiment, the same dipole magnet as in the former A3 experiment will be used, with slight changes in the geometry of its pole tips. Since the y-component of the magnetic field is absolutely dominant, the spins precess in the x-z plane. The resulting transverse neutron polarization behind the magnet is given by the superposition

$$P_\perp(\chi) = P_x\cos\chi - P_z\sin\chi =: P_0\sin(\chi-\chi_0) \tag{6}$$

with

$$P_0 = \sqrt{{P_x}^2+{P_z}^2} \quad . \tag{7}$$

The transverse polarization component, $P_\perp(\chi)$, varies with the magnetic field strength, and thus the corresponding asymmetry $A_\perp(\chi)$ in the second detector wall. For the particular case of vanishing transverse polarization, $P_\perp(\chi_0)=0$, after spin precession by the angle χ_0, the neutron electric form factor can be experimentally determined from

$$\tan\chi_0 = \frac{A_x}{A_z} = \frac{P_e\mathcal{A}_{\rm eff}P_x}{P_e\mathcal{A}_{\rm eff}P_z} = -\frac{1}{\sqrt{\tau+\tau(1+\tau)\tan^2\vartheta_e/2}}\cdot\frac{G_{E,n}}{G_{M,n}} \quad . \tag{8}$$

In the asymmetry ratio, both P_e and $\mathcal{A}_{\rm eff}$ cancel out. Their absolute values affect only the statistical error of the determination of the zero crossing point χ_0, but not its absolute value. The electron beam polarization has to be monitored, in order to detect possible changes with time. This will be done with the Møller polarimeter, which has recently been installed in the spectrometer hall.

The proposed experiment will measure the neutron electric form factor at significantly higher four-momentum transfers than in the previous $\mathrm{D}(\vec{\mathrm{e}},\mathrm{e}'\vec{\mathrm{n}})\mathrm{p}$ experiments. Since the cross section of the quasielastic $\mathrm{D}(\vec{\mathrm{e}},\mathrm{e}'\vec{\mathrm{n}})\mathrm{p}$ reaction roughly falls with $(Q^2)^{-2}$, correspondingly higher beam currents of about 10 μA and a 5 cm thick LD_2 target must be used in order to achieve the required statistical accuracy. The neutrons have to be detected at forward angles ($\vartheta_n \simeq 25.6° - 36.9°$), where the detectors are exposed to a substantial electromagnetic background. This required the construction of a new neutron polarimeter.

3 Neutron polarimeter

The neutron polarimeter was optimized for background compatibility at luminosities up to $2 \cdot 10^{37}$ $\text{cm}^{-2}\text{s}^{-1}$. The background was studied in a dedicated test experiment with realistic precession magnet geometry and field, using beam currents up to 15 μA on a 5 cm LD_2 target. It was found that, even at the most forward angles, the background rate in the scintillators is low enough to allow safe neutron identification. In order to reduce low-energetic background, a lead shield (5 cm thick) is required between target and magnet.

The geometry of the two scintillator walls is determined by the maximum allowed counting rates in the single detector elements and the necessary angular and time-of-flight resolution for neutron detection. The neutrons are measured in a first wall which is segmented into 30 plastic scintillator bars of size $80 \times 7.5 \times 5.0$ cm^3. They are grouped in pairs in the way shown in the lower part of Figure 3. In order to suppress charged background particles, 15 individual veto detectors with 10 mm thickness are placed in front of them.

The measurement of the neutron polarization requires the azimuthal angular distribution of neutrons scattered in the first scintillator wall. In order to determine the neutron scattering angles (Θ_n', Φ_n'), the neutrons are detected once again in a second wall, which consists of 24 scintillators ($180 \times 20 \times 10$ cm^3), and appropriate veto detectors.

The test experiment showed that a low enough background rate in the second wall can only be achieved by placing its scintillation counters above and below the region defined by the magnet gap, i.e. without direct view to the target.

The efficiency for double neutron detection was estimated in a simulation [12] based on the known interaction rate and angular distribution of neutrons in the scintillators. The value $\varepsilon \simeq 1.66 \cdot 10^{-3}$ in the range of useful analysing power is of the same order as the experience from former Mainz experiments [1, 2].

The use of spectrometer A for the detection of the electron energy E_e' and its scattering angles ϑ_e, φ_e permits a much better resolution than the formerly used lead glass array. The scintillators of the first wall have a width of only 5 cm, providing a good resolution of the neutron angles ($\sigma(\vartheta_n) = 3\,\text{mrad}$, $\sigma(\varphi_n) = 8\,\text{mrad}$). With these five observables, the kinematics of the $\mathrm{D}(\vec{\mathrm{e}}, \mathrm{e}'\vec{\mathrm{n}})\mathrm{p}$ reaction can already be completely reconstructed. Furthermore, the neutron time of flight will be measured as well, allowing additional checks in the data analysis. Thus a systematic error is expected of the same size as the statistical one.

4 Kinematics

We propose to measure the neutron electric form factor at two different Q^2 of 0.6 and 0.8 $(\mathrm{GeV}/c)^2$ The corresponding kinematics are summarized in Table 1.

Longitudinal beam polarization requires a beam energy of $E_e = 854.4$ MeV. The scattered electrons are detected in spectrometer A with a solid angle of 21 msr. On the opposite side of the beam line the dipole magnet will be installed at 3 m distance from the target. The first scintillator wall will be placed at a distance of 6 m from the target, the second one at 8.5 m.

Setup	$Q^2/(\frac{\mathrm{GeV}}{c})^2$	E'_e/ MeV	ϑ_e	ϑ_n	T_n/ MeV	β_n
I	0.6	535.5	69.83°	36.86°	319.5	0.67
II	0.8	429.0	95.19°	25.55°	426.0	0.73

Table 1: Particle energies and scattering angles at the proposed four-momentum transfers ($E_e = 854.4$ MeV).

5 Counting rate estimate and beamtime request

The counting rate estimate is based on the following assumptions:

- The Rosenbluth cross section of the $\mathrm{D}(\vec{\mathrm{e}},\mathrm{e}'\vec{\mathrm{n}})\mathrm{p}$ reaction at the two values chosen for the momentum transfer is [12]

$$\begin{aligned} \frac{d\sigma}{d\Omega}(Q^2 = 0.6\ \ (\mathrm{GeV}/c)^2) &= 2794 \text{ pb/sr} \\ \frac{d\sigma}{d\Omega}(Q^2 = 0.8\ \ (\mathrm{GeV}/c)^2) &= 696 \text{ pb/sr} \end{aligned}$$

- The LD_2 target cell is 5 cm long, yielding a density of $n_K = 2.44 \cdot 10^{23}$ cm^{-2}. An average beam current of $I = 10$ μA can be achieved. A maximum of 15 μA should be possible according to detector tests (see section 3).

  This leads to a luminosity $\mathcal{L} = 1.5 \cdot 10^{37}$ cm^{-2}s^{-1} $= 55$ fb^{-1}h^{-1}.

- For the electron spectrometer A we have to use a collimator with an angular acceptance of $\Delta\Omega_e = 21$ msr due to the long target cell.

- The overall efficiency of the neutron polarimeter is $\varepsilon \simeq 1.66 \cdot 10^{-3}$, taking into account the distribution of the neutrons after the scattering in the first wall, the detection efficiency of the scintillators, and the partial absorption of neutrons in the lead shielding (5 cm) between target and polarimeter. This number is supported by the results obtained in Ref. [12].

The coincidence counting rates are obtained through

$$\dot{N} = \frac{d\sigma}{d\Omega} \cdot \mathcal{L} \cdot \Delta\Omega \cdot \varepsilon \ . \tag{9}$$

Our proposal is to measure $G_{E,n}$ at two values of momentum transfer, $Q^2 = 0.6\ (\mathrm{GeV}/c)^2$ and $Q^2 = 0.8\ (\mathrm{GeV}/c)^2$. The Q^2 intervals which are covered at these values are determined by the angular acceptance of spectrometer A (see Table 2). The electron momentum and neutron scattering angle will then fit into the momentum acceptance of the spectrometer and the angular acceptance of the neutron polarimeter, respectively. The statistical error of the asymmetry measurement depends on the number N of detected events via the relation [13]

$$\frac{\Delta G_{E,n}}{G_{E,n}} = \frac{\Delta A}{A} = \left(\sqrt{N} \cdot P_e \cdot P_x \cdot \mathcal{A}_{\mathrm{eff}}\right)^{-1} \ . \tag{10}$$

We aim for a statistical error of $\Delta G_{E,n}/G_{E,n} = 5\%$. With a beam polarization $P_e = 75\%$, an x component of the neutron polarization $P_x = 0.17$, and an effective analysing power $\mathcal{A}_{\mathrm{eff}} = 0.2$, one obtains $N = 620000$. This leads to the measuring times summarized in table 2. The systematic error is expected to be of the same order as the statistical one.

Setup	$Q^2/(\frac{\mathrm{GeV}}{c})^2$	$\frac{d\sigma}{d\Omega}/\mathrm{pb\,sr}^{-1}$	$\dot{N}/\mathrm{h}^{-1}$	beamtime/h
I	0.6 ± 0.040	2794	5340	116
II	0.8 ± 0.027	696	1330	466

Table 2: Expected counting rates and measuring times.

Furthermore, the following additional time will be required:

- 7 days without beam for first setup of the experiment in the spectrometer hall
- 24 hours for setup with beam and trigger adjustment
- 24 hours for calibration runs
- 48 hours with liquid hydrogen (proton) target to determine the rate of protons misidentified as neutrons in the polarimeter
- 3 days without beam for changeover to the second Q^2 setup

- 8 hours setup with beam for second Q^2
- 12 hours for intermediate polarization measurements with the Møller detector (30 minutes every 24 hours)

The overall beamtime request summarizes to 698 hours.

References

[1] C. Herberg et al., *Eur. Phys. J.* A **5**, 131 (1999)

[2] M. Ostrick et al., *Phys. Rev. Lett.* **83**, 276 (1999)

[3] I. Passchier et al., *Phys. Rev. Lett.* **82** 4988 (1999)

[4] T. Eden et al., *Phys. Rev. C* **50**, R1749 (1994)

[5] J. Becker, submitted to *Eur. Phys. J.*

[6] D. Rohe et al., accepted for publication in *Phys. Rev. Lett.*

[7] S. Platchkov et al., *Nucl. Phys. A* **510**, 740 (1990)

[8] H. Arenhövel, *Z. Phys. A* **331**, 123 (1988); *Z. Phys. A* **334**, 363 (E) (1989)

[9] R. G. Arnold et al., *Phys. Rev. C* **23**, 363 (1981)

[10] T. N. Taddeucci et al., *Nucl. Instrum. Methods A* **241**, 448 (1985)

[11] K.I. Blomqvist et al., *Nucl. Instrum. Methods* A **403**, 263 (1998)

[12] M. Seimetz, diploma thesis, Institut für Kernphysik, Mainz 1999

[13] D. Eyl, dissertation, Institut für Kernphysik, Mainz 1994